ELSEVIER

Analytica Chimica Acta 337 (1997) 233–252

ANALYTICA CHIMICA ACTA

Review

Accurate quantification of quartz and other phases by powder X-ray diffractometry

Vernon J. Hurst[a,*], Paul A. Schroeder[a], Robert W. Styron[b]

[a]*Geology Department, University of Georgia, Athens, GA 30602-2501, USA*
[b]*Mineral Resource Technologies, Atlanta, GA, USA*

Received 30 April 1996; revised 27 August 1996; accepted 28 August 1996

Abstract

The 33 parameters that affect accuracy of quantitative analysis by X-ray powder diffractometry can be grouped as (1) Instrumental or systematic, (2) Inherent properties of the analyte, or (3) Parameters related to preparation and mounting of powders. The effect of each on diffraction intensity is summarized. An optimal value or range is given for instrumental parameters. Evaluation of inherent parameters of the analyte and optimization of those related to preparation and mounting of powders are discussed. Published methods are briefly reviewed. Their reported detection limits for crystalline silica are well below what can be reliably determined in natural and industrial products if one or more critical parameters are neglected, as the size and shape of coherent diffraction domains. An addendum illustrates practical consideration of major parameters during routine analysis for quartz.

Keywords: Crystalline silica; X-ray diffraction; Quantification; Fly ash; Quartz; Review

1. Introduction

There is increasing interest in determining and monitoring quartz and other forms of crystalline silica in commercial and industrial bulk products which are or might yield respirable dusts. For more than a century silica has been recognized as a cause of fibrosis (silicosis) which may lead to chronic lung ailments. It is regulated in USA by the Occupational Safety and Health Administration and the Mine Safety and Health Administration for worker exposure to respirable dust. The National Toxicological Program lists respirable crystalline silica in three natural and industrial forms as "reasonably anticipated to be carcinogenic". A currently enforced Hazard Communication Standard requires that all products containing 0.1% or more of these three forms be labelled as "Hazardous". This regulation poses a dilemma because the 0.1% threshold is beyond the capability of methods currently in use except when they are restricted to a well characterized and essentially invariant bulk material. When applied generally, they cannot be relied on to detect

* Corresponding author.

PII S0003-2670(96)00425-4

all forms of crystalline silica at a concentration of even several percent.

Chemical methods are not sufficiently specific for silica in each of its crystalline states [1]. A suitable quantification method must be capable of identifying particular Si–O arrays (minerals) and accurately measuring a parameter specific for each. Both requirements are complicated by the fact that crystallites/grains of silica (and other materials) generally are inhomogeneous on a microscale. Defects and/or microfractures break up grains into smaller domains differing in orientation and internal order. The smaller the domains and the greater their misorientation, the more difficult is quantification.

Optical methods, differential thermal analysis, Infra-red absorption, and Fourier Transform Infrared Spectroscopy can measure physical properties that relate to the kind and orderliness of atomic arrays, but are not as specific, reproducible, and sensitive at low concentrations as X-ray diffraction (XRD).

Terms like "amorphous, well- and poorly-crystallized" are often misleading as applied to diffraction patterns. Broad, low, poorly resolved peaks and missing reflections, sometimes regarded as indicative of poor crystallinity, can be due as well to smallness and misorientation of coherent diffraction domains (CDDs).

XRD can identify minerals with well ordered CDDs as small as several hundredths of a micron. When CDD size is optimal, ~5–0.2 microns, diffraction intensity is proportional to concentration. When coarser or finer, this relationship can be adversely modified by primary–secondary extinction or fine CDD effects, respectively. Examination of XRD peaks of the analyte can indicate the likelihood of a quantification problem. The first noticeable small CDD effects are peak broadening and reduced intensity. No diffraction peak for the analyte might indicate that none is present or that its CDDs are too fine to yield XRD data. The choice between these possibilities can be made from electron diffraction patterns. When the material to be analyzed has not been well characterized previously, or its XRD pattern suggests the presence of CDDs smaller than 0.2 μm, electron microscopy can be used to measure actual CDD size, size distribution, and intra-CDD order. Two crystalline silica polymorphs, moganite and cristobalite, often found in natural and industrial products, commonly show wide variability in CDD size and internal order. Reliable quantification

Table 1
Parameters that affect the accuracy of diffraction intensity measurement

A. Instrumental or systematic parameters	B. Inherent properties of the phase (Compound/Mineral)	C. Parameters related to the preparation and mounting of powders
1. X-ray source intensity, kV and mA settings of the generator	16. Structure factor, F	23. Size distribution of coherent diffraction domains
2. Scan rate	17. Multiplicity	24. Preferred orientation
3. Chopper increment	18. Long-range order so-called "crystallinity"	25. Sample homogeneity
4. Divergence slit width	19. Absorption factor, μ, and transparency	26. Average mass attenuation coefficient, $\bar{\mu}$
5. Receiving slit width	20. Primary extinction, belongs in both the B and C categories	27. Microabsorption
6. Detector deadtime	21. Secondary extinction, belongs in both the B and C categories	28. Size of exposed sample surface
7. Lorentz-Polarization factor	22. Temperature factor	29. Thickness of the powder
8. Counting statistics		30. Sample surface characteristics
9. Total sample surface irradiated		31. Powder packing and transparency
10. Sample displacement, actual and effective. The latter belongs partly in C category		32. Methods for making powder mounts
11. $K_{\alpha 2}$ stripping or not		33. Choice of internal standard(s)
12. Degree of data smoothing		
13. Method of peak area measurement		
14. Background and choice of subtraction method		
15. Parameters of special software routines, as deconvolution		

necessitates an intensity vs. concentration curve established from standards having CDD size and intra-CDD order closely similar to those of the analyte and close accounting of background.

Several applications of powder XRD to phase analysis have been published. Better examples [2–10,24,25] report careful measurements, but none have dealt explicitly with all factors that influence diffraction intensity.

The accuracy of quantitative powder XRD depends on how precisely diffraction intensity can be measured and, generally less appreciated, how intensity data are interpreted. All of the intensity-affecting parameters in Table 1 should be considered. Much background information is available from a long list of technical papers, a recent book of reviews [11] and a special issue of Analytica Chimica Acta [26]. This paper aims at highlighting critical instrumental parameters and sample-handling procedures. A few aspects of measurement not covered adequately in the literature are discussed. The addendum on quantification of quartz exemplifies consideration of more critical parameters and how some may be obviated by examination of background information on the analyte and its matrix.

2. Measurement of diffraction intensity

A rote set of factors chosen by a knowledgeable person from Table 1 can be used to quantify a mineral/compound, provided its physical properties are invariant and its matrix is always the same. When diverse samples are to be analyzed, especially from diverse sources, considerable variation can be expected, and all parameters in Table 1 should be considered.

2.1. Systematic parameters

2.1.1. X-ray intensity at the source

When the diffractometer is well aligned and all elements of the system are functional, early control choices of the operator are kV and mA settings for the generator. Higher settings to increase peak (and background) intensity and improve counting statistics can be weighed against the possibility of shortening tube life. While low settings are satisfactory for some qualitative uses, they are antithetic to accurate measurement of both d-spacings and peak intensities. Higher settings, like 45 kV and 40 mA should be employed for accurate quantitative work, when the common 2000 watt, fine focus, Cu-target tube is used.

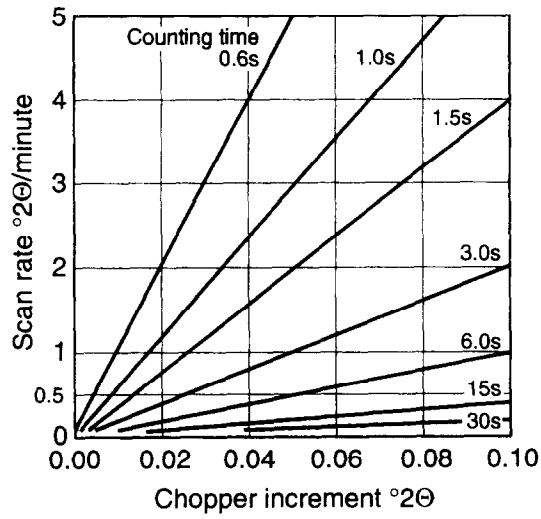

Fig. 1. Count time in relation to scan rate and chopper increment. Count time × intensity = number of counts (Fig. 4).

2.1.2. Scan rate and chopper increment

These determine count time (Fig. 1). Chopper increment is the 2Θ-interval over which counts are averaged for each data point. Count time × intensity (counts/time unit) = total counts/increment. This and the ratio of peak/background determine probable counting error, which usually is a major part of intensity measurement error.

These parameters are important not only for quantitative analysis but also for routine phase identification and d-spacing measurement. Data obtained at a scan rate of $4°2\Theta\ min^{-1}$ generally resolve fewer peaks than data collected at a rate of $1°2\Theta\ min^{-1}$. Likewise, the accuracy of d-spacings measurement at the higher scan rate is significantly less. At a high scan rate, even strong peaks of a minor phase may be undetectable. Probable error increases rapidly with increasing scan rate.

2.1.3. Divergence slit width

This limits divergence of the X-ray beam from the source. Width hardly affects relative peak intensities,

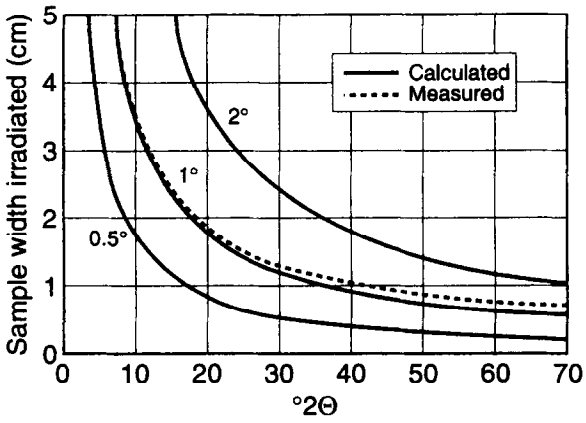

Fig. 2. Sample length irradiated as a function of 2Θ and divergence slit width for the regular sample holder of XDS-2000.

if the slit is fixed and the specimen completely intercepts the X-ray beam. Irradiated length of the specimen varies with divergence slit width and 2Θ. For example, the irradiated area of a sample mounted in the regular holder for Scintag XDS-2000 is about 25 mm wide and 25 mm long. This surface completely intercepts the X-ray beam when a 1° divergence slit is used and 2Θ is 13° (Fig. 2). At lower 2Θ, the sample intercepts only part of the beam, resulting in reduced beam intensity per unit of sample surface and the likelihood of increased background due to scatter. At higher 2Θ, the sample intercepts all of the beam but less and less of the sample surface is irradiated, and the likelihood of counting error increases. The choice of a fixed divergence slit involves compromise between irradiated sample length, diffraction intensity, and counting statistics. A 1° slit is a reasonable compromise for the 10–30°2Θ range. The theta-compensating divergence slit on some diffractometers was designed to lessen high-angle intensity loss and low-angle background. It gives a constant specimen irradiation length, but intensities obtained with it do not agree, of course, with those obtained with a fixed divergence slit.

2.1.4. Receiving slit width

Increasing the width of this slit generally increases peak height and width and decreases resolution of the peak profile, especially if slit width exceeds beam width. The latter depends upon axial divergence from the source, the collimator, and width of the divergence slit. For optimal intensity and resolution, the receiving slit should be >0.2° and about the same as beam width.

In a Θ–Θ scan, rotation of the X-ray source and detector to new angles may bring new regions of a mosaic crystal into reflecting orientation. The net effects of diffraction from many very small mosaic domains [12] differing slightly in orientation rather than diffraction from a large single crystal are a decrease in extinction and an increase in intensity. For accurate integrated intensity measurements on coarse grains, it is essential that they have mosaic structure and that the slits be set wide enough to obtain the entire reflection from every mosaic domain. If the receiving slit is increased until intensity above background is constant for a large mosaic single crystal, its width will be more than adequate for a powder, because a large crystal generally has more mosaic spread than a small grain. Smaller receiving slits that hardly sacrifice resolution can be used for powders of optimal size.

2.1.5. Detector deadtime

When measured count rate is not directly proportional to the photon rate entering the detector, the detector is non-linear and is said to have deadtime, which has the effect of increasing the intensity of weaker lines. Most diffractometers can satisfactorily handle count rates up to 100 000 counts sec^{-1} without serious deadtime error.

To check on whether deadtime might cause intensity error, first measure the intensity of the strongest line at the X-ray tube current to be used for a given set of measurements, then measure the line a second time at half the tube current used for the first measurement. If the second measurement is more than half of the first, detector deadtime is the probable cause.

2.1.6. Lorentz-Polarization factor

Diffraction polarizes the X-ray beam by an amount that depends upon the angle of scatter. Possible error due to polarization is corrected by the Polarization Factor. The Lorentz Factor is essentially a time-reflection factor. For a given diffractometer system, the combined Lorentz-Polarization correction is a ready option. Its variation with Θ is shown in Fig. 3. Peaks used for intensity measurement should not be on a steep portion of the L-P curve.

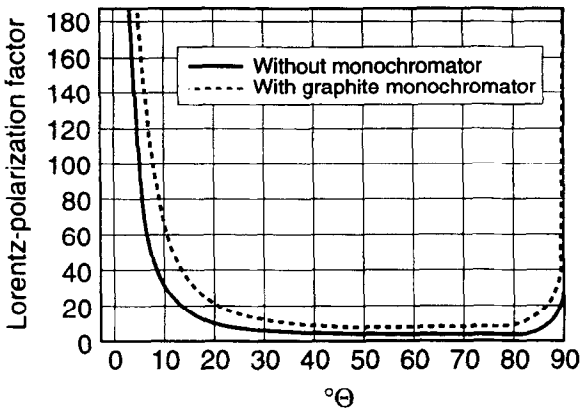

Fig. 3. How the Lorentz-Polarization factor varies with Θ.

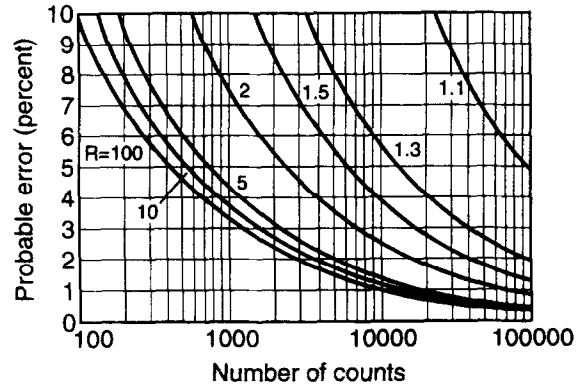

Fig. 4. Probable error in relation to total number of counts and peak/background ratio, R [19].

2.1.7. Counting statistics

The precision of raw intensity data can be limited more by counting statistics than any other single parameter except preferred orientation. The probable error of peak intensity measurement varies with the total number of counts and the ratio of total to background counting rate (Fig. 4), both of which depend upon scan rate and chopper increment (Fig. 1). For a chopper increment of 0.01 degree and a scan rate of $2°2\Theta\ min^{-1}$, for example, count time per increment is only 0.3 second. If counting rate at the top of the peak is 1000 counts sec^{-1}, then the total number of counts at the top of the peak is only 300. If the peak/background ratio (R) is large, the best precision attainable at this counting rate is about ±4%, as shown in Fig. 4. If R=1.5, probable error exceeds 10%; it can be dropped to 5% by decreasing

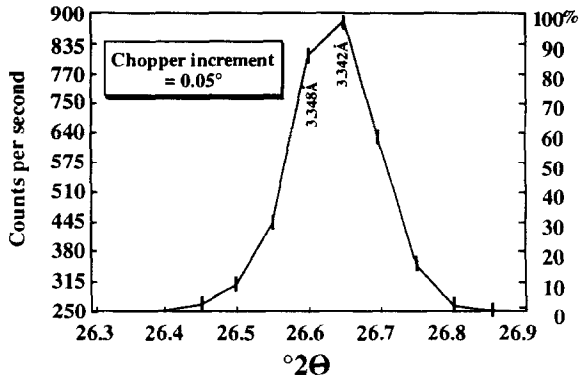

Fig. 5. Portion of a diffractogram magnified to show how peak resolution depends upon chopper increment, marked as breaks in the intensity curve, and scan rate. Peak intensity obtained by deconvolution is better than maximum recorded intensity.

the scan rate to $0.2°2\Theta\ min^{-1}$. Further improvement in peak intensity measurement is possible by smoothing the top of the peak over 15 increments to better establish its height and by averaging the background over hundreds of increments on both sides of the peak. Alternatively, the goniometer can

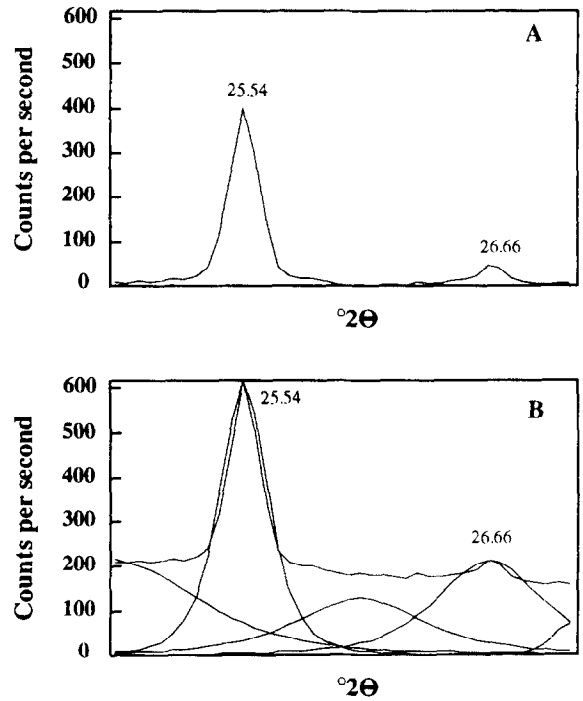

Fig. 6. Comparison of peak deconvolution with (A) peak background set along the average background trace and (B) set at zero.

be set at the top of the peak to accumulate a sufficient number of counts for the desired precision and set on two or more points, for longer times, to obtain equally precise measurement of background. A possible disadvantage of the first alternative is that peak position can vary, for several reasons, necessitating a pre-scan to accurately locate the top (Fig. 5); at least two additional long counts will be required to accurately establish background, particularly when the proportion of the unknown is small. A possible disadvantage of the second alternative is that part of the measured peak intensity might relate to another mineral not detectable from a limited scan range and from incoherent scatter. The best alternative is to use total peak area as the measure of intensity, or integrated intensity. A practical way to do this is to deconvolute the raw data file, using computer software. The zero for background is set along the average of the background trace (Fig. 6). It is not set at zero intensity because much of the diffraction intensity between zero and the background trace is from incoherent scatter.

2.1.8. *Total surface irradiated*

This factor is limited by the design of the diffractometer, the divergence slit, and 2Θ (Fig. 2). For quantitative accuracy the irradiated surface should be maximal, for better counting statistics, an important fact is sometimes overlooked.

2.1.9. *Sample displacement error*

Displacement of the sample with respect to the focal plane of the goniometer not only changes the measured value of *d* (Fig. 7A), but also decreases diffraction intensity. Displacement error increases as 2Θ decreases, and increases rapidly as 2Θ falls below 20° (Fig. 7B). Actual displacement can be caused by misalignment of the goniometer, an uneven sample surface, or a smear mount when powder does not completely cover the slide. Effective displacement,

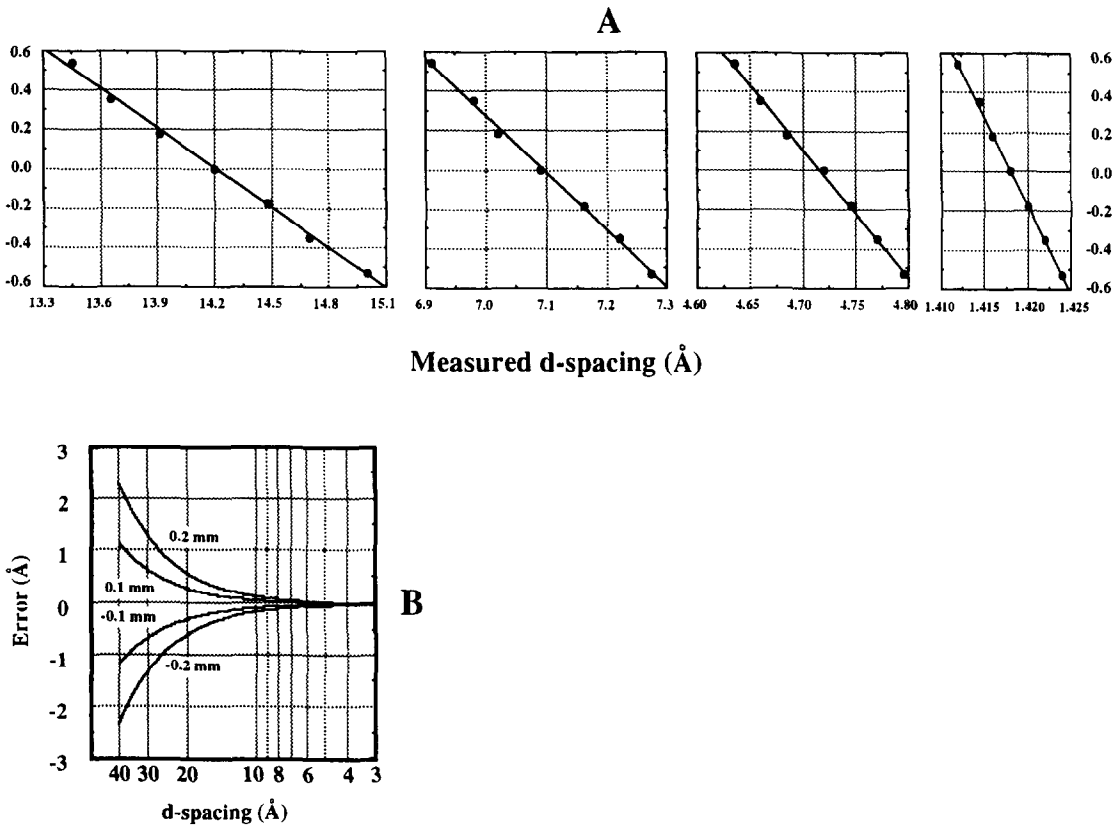

Fig. 7. The d-spacing measurement error resulting from sample displacement. 7B shows how rapidly error increases at low 2Θ.

sample transparency, can be a consequence of low μ, $\bar{\mu}$, or high sample porosity. For further discussion see section 2.3.9.

2.1.10. $K_{\alpha 2}$ stripping

At low values of 2Θ, α_1 and α_2 peaks are completely overlapped. If α_2 stripping is invoked, net intensity is reduced by one-third. This reduction vanishes toward higher 2Θ as α_1 and α_2 peaks are resolved.

2.1.11. Degree of data smoothing

The option to smooth raw data and how much should be considered case-by-case. It suppresses peak intensity and may affect the accuracy of intensity measurement. Peak area measurement is discussed above in section 2.1.7.

2.1.12. Background and method of subtraction

Background can be due to one or more of the following causes:

1. Fluorescent radiation emitted by the specimen.
2. Diffraction of a continuous spectrum of wavelengths.
3. Diffraction and scattering from materials other than the specimen, as collimator, specimen binder or enclosure, air.
4. Diffuse scattering from the specimen itself:
   a) Incoherent (Compton modified) scattering, which increases as atomic number decreases, and thus may be high when light elements are present.
   b) Coherent scattering:
      i) Diffuse scattering due to various crystallite imperfections: any disorder in arrangements of atoms or mechanical strain. Less ordered solids like glass cause intense diffuse scatter.
      ii) Associated with every diffraction maximum are N-1 subsidiary, low-intensity maxima which contribute to background (Table 2, Fig. 9).
      iii) Temperature-diffuse scattering, which is more intense with soft materials having a low melting point, but generally is small.

Whether to opt for background correction depends on its cause. If the predominant cause is 3 or 4-(a), do, and if 4-(b)ii, do not invoke automatic correction. This option should be carefully considered, case by case. Subtraction of background without using the routine option is sometimes better, as mentioned in the section on "Counting Statistics."

Table 2
Symbols and definitions

A	amplitude of the diffracted wave
a,b,c	unit cell axes
CDD	coherent diffraction domain
d	d-spacing
F	structure factor
M	multiplicity
micron=micrometer=0.001 mm	
μ	linear absorption coefficient of a phase
$\bar{\mu}$	mass absorption coefficient of a powder
N	number of unit cell repeats in a give reciprocal lattice direction, i.e., normal to the set of diffracting planes
Θ–Θ configuration	x-ray source and detector both rotate about a fixed sample
RIR	Reference Intensity Ratio [4]
$\|S\|^2=\sin^2 Nu\pi/\sin^2 u\pi$, a one-dimensional representation of the interference function	
SEM	scanning electron microscope
T	temperature factor
TEM	transmission electron microscope
u	any fraction of the distance between two consecutive reciprocal lattice points
XRD	x-ray diffraction

2.2. *Inherent properties of the phase (compound or mineral)*

2.2.1. Structure factor, F

This factor is determined by the kinds of atoms in an ordered structure and the coordinates of each in the unit cell. Its absolute value, $|F|$, is the amplitude of the resultant wave from scatter by all atoms in the unit cell in a given (hkl) direction. Diffraction intensity is proportional to $|F_{(hkl)}|^2$.

2.2.2. Multiplicity

All crystals have a form with at least two faces. The maximum number of equivalent faces in a form increases with symmetry, up to 48 in cubic crystals. The number of sets of equivalent planes contributing to the same reflection enters the intensity equation as the multiplicity factor, M, which is the number of

different planes in the form having the same d-spacing.

2.2.3. Long-range and short-range order (so-called "crystallinity")

Absolute intensity is a consequence of order and symmetry of atomic arrangement, directionality of strong bonding, atomic scattering factors, and CDD size. Atomic scattering factors increase with atomic weight. The higher scatter of heavier atoms with short-range order, however, may be exceeded by an array of lighter elements with long-range order. The initial range of order of a mineral/compound originated during formation and growth, but commonly has been changed by subsequent chemical degradation, mechanical strain, or recrystallization, or by sample preparation. Long-range order extends over more than ≈200 unit cells. Reflecting planes normal to a direction of long-range order give a sharp, narrow, symmetric peak. Short-range order extends over fewer than ≈50 unit repeats. Reflecting planes normal to a direction of short-range order give a lower and broader peak, and contribute inordinately to background. As range of order decreases, diffraction peaks lower and broaden until they merge with background. Whether CDDs are equant or irregular in shape can be deduced from indexed (h00), (0k0), and (00l) reflections. No diffraction peak is obtained when range of order is less than ≈5 unit repeats.

Diffraction intensity from a unit cell is proportional to the square of the amplitude of the wave diffracted from it, $|F_{(hkl)}|^2$. This amplitude increases in proportion to N^2 (Table 2). Absolute intensity would increase asymptotically with range of order if the countering effects of primary and secondary extinction and other factors did not increase at the same time.

The terms crystallinity and amorphous (to X-rays) have been used a long time to refer vaguely to degree and range of order (or presumed existence of total disorder). Convenient methods for measuring these characteristics were not generally available, and brief expressions for them were still to be defined. Lattice imaging enables direct observation and rapid measurement of CDD size and shape. If electron diffraction patterns reveal broadening or streaking incompatible with CDD size distribution and shape, it can be attributed to intra- or inter-crystallite disorder, the nature of which can be identified by analysis of electron diffraction patterns. When cost considerations rule out an evaluation of CDD size distribution and ordering, any quantification based on a physical property of an atomic array (mineral) must be regarded as provisional, subject to as much uncertainty as can be expected from unevaluated parameters. For reliable quantification, CDD size distribution and ordering of the analyte must be very similar in the sample to be analyzed and in the set of standards from which the concentration versus intensity curve was derived. When all particles of the powdered sample are within the optimal range, all diffraction peaks from the sample are narrow, and background is very low, careful quantification is apt to be reliable. When the analytical peak shows broadening, CDD size distribution and degree of order should be evaluated, else they might result in large analytical error.

2.2.4. Absorption factor, μ

This factor is the linear absorption coefficient of a solid phase for the X-ray wavelength used, the number by which calculated intensity must be multiplied to allow for absorption. It depends upon the geometry of the diffraction instrument. For a powder diffractometer, the absorption factor equals $1/2\mu$ and is independent of Θ. Still, the larger the absorption coefficient of powder particles, the lower the intensity of diffracted beams, other things being equal. Notably, μ absorption decreases the intensities of all diffracted beams by the same factor and therefore does not enter into the calculation of *relative* intensities [12]. When μ is low, the X-ray beam penetrates deeper into the sample. The result is effective sample displacement error.

2.2.5. Primary and secondary extinction

Powder particles consisting of one or more coarse CDDs may diffract more weakly than would be expected from perfect crystal theory and from its linear absorption coefficient, μ. The difference between observed and expected intensity may arise from *primary* and *secondary extinction* which act as additions to the regular absorption coefficient. Primary extinction results when a once-diffracted beam is rescattered back into the incident beam direction and, being out of phase, destructively

interferes. Secondary extinction results when a crystallite oriented for diffraction is below other crystallites that diffract, when the energy of the beam striking it has been weakened by scatter from overlying crystallites. An additional absorption factor, microabsorption, comes into play when the powder sample is coarser than about 5μ and contains two or more substances having very different mass absorption coefficients. Then diffraction intensity decreases in relation to the relative proportions of the substances and their mass absorption coefficients. While the linear absorption factor, $1/2\mu$, may be regarded as independent of Θ, owing to geometry of the diffractometer, and a constant in the calculation of relative intensities, extinction and microabsorption factors are not constants. Only to the extent that they are inherent properties of the analyte and the powder is prepared reproducibly can they be neglected during the calculation of relative intensities. In any case, primary extinction is less for higher-angle reflections, and secondary extinction is greater for strong than for weak reflections. Notably: *primary extinction and secondary extinction, as well as microabsorption, are negligible for powders finer than 5 microns.*

2.2.6. Temperature factor

The atoms in a structure undergo thermal vibration about their mean positions even at very low temperatures. The amplitude of this vibration increases as temperature increases. The results are (1) expansion of the unit cell with attendant changes in the 2Θ positions of diffraction lines, (2) decreasing diffraction intensities, and (3) increasing background scatter.

In routine work, thermal expansion can be neglected. For accurate measurement of d-spacings, however, temperature has to be controlled. A change of one degree generally affects the 5th decimal place, and a rise of several degrees affects the 4th decimal place. In quartz, for example, an increase in room temperature of one degree increases its *c*-spacing 0.00005 Å and the increase goes up rapidly as temperature rises.

The intensity of a diffracted beam decreases as temperature rises and, at constant temperature, decreases more at higher angles. In intensity calculations allowance can be made for these effects by using a temperature factor, $(\exp)^{-2M}$, by which calculated intensity is multiplied to allow for thermal vibration of atoms. $M = B(\sin\theta/\lambda)^2$. B is hard to determine accurately, because it includes the effects of not only thermal vibration but also structural and substitutional disorder and the elastic constants of the crystal. Typical values for most silicates are about 1.4 for cations and 1.8 for oxygen. Uncertainty in the value of B does not lead to large error if calculated intensities are restricted to low-angle peaks. For example, at 50°2Θ ($Cu_{k\alpha}$) a difference in B of 0.4 amounts to a difference in atomic scattering amplitude of less than 2%; at lower angles the difference is less. Very large values of B may have to be used for organic molecules, like those arrayed in interlamellar spaces of smectite. For ethylene glycol in these spaces the value B=11 has been used [13].

The amplitude of thermal vibration depends not only on temperature but also on the elastic constants of the crystal. It is greater for materials that are softer and have a lower melting point. For some materials it is great even at room temperature [12]. For example, thermal atomic vibration in lead at 20°C reduces the intensity of the highest angle line observed with $Cu_{k\alpha}$ radiation (at about 161.2°2Θ) to only 18% of the value for atoms at rest ($(\exp)^{-2M} = 0.18$).

The quantity M can be approximated for a given material by careful diffraction intensity measurement at constant temperature. When the temperature factor is neglected, the error in intensity measurement caused by thermal vibrations can be minimized by using peaks below 50°2Θ. For additional information, see [14].

2.3. Parameters related to preparation and mounting of powder

2.3.1. Coherent diffraction domains and their size distribution

A single crystal or particle may consist of one CDD or many (Fig. 8B) and give no visual or microscopic indication. Maximum diffraction intensity is obtained from CDDs of intermediate size, ≈5000–100 unit repeats (≈5–0.1 microns) thick. These are coarse enough for strong N^2A^2 reenforcement (Table 2) and fine enough to obviate primary and secondary extinction and microabsorption, without inducing serious line broadening and intensity reduction.

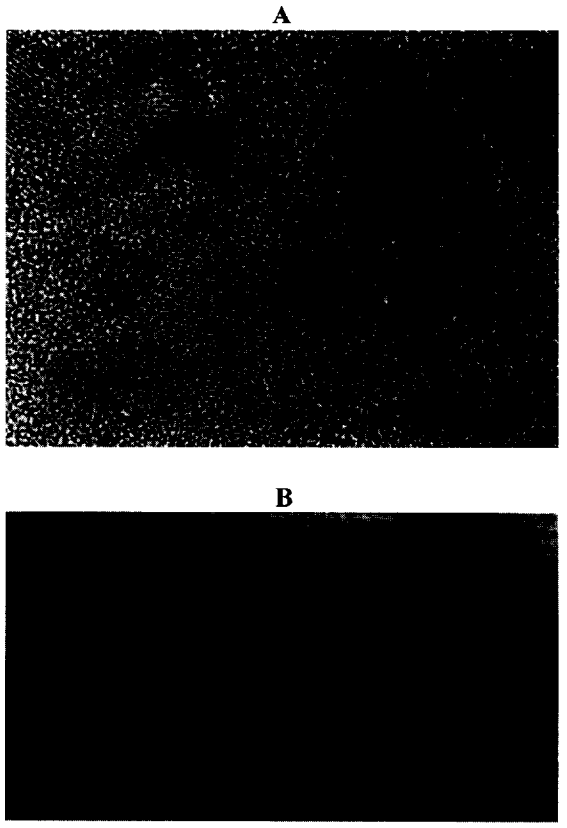

Fig. 8. High resolution TEM photographs, magn. ≈3 million, illustrating short-range order. (A) Silicon; within coherent diffraction domains, 3.13 Å repeats in the [111]* direction are well resolved. For the CCD at the arrow, N=7, for the larger CDD below it, N=35 (photo by J.B. Posthill). (B) Kaolinite from the Prim Mine, Georgia. The 7.16 Å repeat in the c* direction is regular for 7 layers, the visible misorientation between packets reduces (001) intensity.

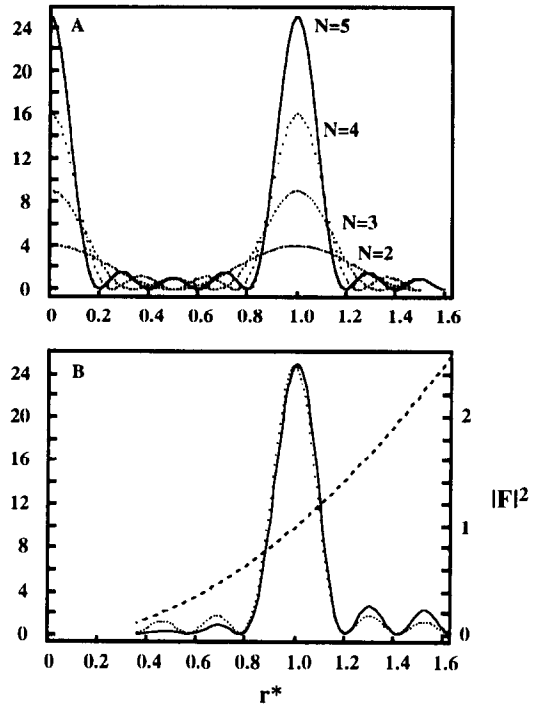

Fig. 9. (A) Graph of the interference function showing how peak height and shape vary with N.(B) A theoretical line-profile for N=5 is the solid line. The interference function is the dotted line. An arbitrary structure factor curve is the dashed line. Its positive slope is consistent with a shift of the (001) peak to higher 2Θ and increased intensity. If its slope were zero, neither peak position nor intensity would shift [23].

CDDs can be fairly regular in shape (as in Fig. 8B) or complexly interwoven as observed in length-fast chalcedony, a variety of quartz having short-range order. Dark-field TEM images of the latter [15] show pervasive disorder wherein the CDDs appear dendritic.

Diffraction intensity measured with a diffractometer, neglecting lesser factors, is: $I = (L - P)M|F|^2|S|^2$. For one unit cell the amplitude of the diffracted wave is $|F|$. The amplitude of the total wave is proportional to N^2, part of the interference function, S (Table 2). If structural data for the analyte are available, F can be calculated and plotted over the 2Θ range of the analytical peak to be used to show whether peak broadening due to small CDD size shifts the 2Θ position of the peak from its true value, and if, there were a shift, whether it would be in the direction of higher or lower 2Θ (Fig. 9B).

Particles composed of several CDDs may be much coarser than 5 microns and still give maximal intensity, but, when finer than 0.1 micron they always give reduced intensities. If all or most CDDs are smaller than ≈0.005 microns, no diffraction peak will be seen, only a higher-than-normal background. If some are in the range 0.1–0.005 microns, a few low peaks or a very broad hump will be seen above higher-than-normal background. When coarse particles composed of many CDDs of optimal size are comminuted, finer particles with about the same CDD size may be produced, with little or no change in intensity.

The size distribution of CDDs is a core parameter which must be evaluated to some degree in any

procedure for accurate XRD analysis. In some cases, an evaluation based solely on XRD data is sufficient. Such data may show whether there is a problem with fine CDDs and whether the problem is minor or great. Background information on material to be analyzed sometimes can indicate whether a problem with fine CDDs is likely. When CDDs are finer than a few hundreths of a micron, the analysis can be flagged, or aided by supplemental electron microscopy. Past efforts aimed at practical consideration of CDD size have focused on particle size distribution ([16] and others), often very different from CDD size.

By careful grinding as detailed below, all particles of the sample can be reduced to <5 microns, efficiently eliminating any error from long-range order, except when compounds having a very large unit cell are present. They can be recognized from a rapid XRD scan and a computerized search of JCPDS data.

Elimination of error relating to short-range order generally requires more than a particle size analysis. An XRD scan may indicate whether CDDs finer than 0.2 μm are present, except when their internal order is low, but cannot measure their proportion of the sample unless precautions mentioned in the section on "Long-range and Short-range Order" have been taken. To the extent that the analyst knows the origin of the analyte, its crystal chemistry, geochemical behavior, and any special treatment accorded it, he may shorten any post-XRD effort required for accurate quantification. For example, if the analyte is quartz in a natural material that has undergone complete recrystallization, an analyst knowing the geochemistry of quartz would expect only long-range order and no difficulty with preferred orientation. Careful wet grinding, barely enough for all particles to be finer than 5 microns, would be sufficient. If the quartz were in fly ash, an analyst knowing that its diffraction characteristics do not change appreciably during coal combustion would proceed accordingly. If the analyte were cristobalite, the knowledgeable analyst would be aware that short-range order is very expectable for this mineral and would carefully evaluate CDD size distribution before selecting a compromise size range for intensity measurement, a special set of standards, or an alternative quantification procedure. The special standards might not be applicable, of course, to other cristobalite-bearing samples.

If the analyte might be moganite, an analyst knowing that it is characterized by short-range order and is common in many natural materials [17] might anticipate a serious problem with too-fine CDDs and begin with high resolution electron microscopic examination. A check on mineralogical and geochemical background information generally facilitates XRD quantification.

CDD size distribution is easier to evaluate in the <0.2 micron particle size fraction than in coarser fractions. Using TEM with a double-tilt, eucentric stage, an electron diffraction pattern can be obtained in seconds for individual particle identification, and thin edges of fine particles can be checked by lattice imaging for CDD size. A sufficient number of particles can be examined to insure representativeness. Finer particles require no preparational ion milling. Unless their CDD size distribution is found to be very uniform from particle to particle, coarser particles should be milled and examined.

The importance of CDD size has been neglected. A powder of particles finer than optimal gives an intensity-biased quantification less than the actual amount. Error increases as both the proportion of finer CDDs and their fineness increase. In extreme cases, a compound/mineral may be undetectable by diffraction even when it is a major component of the sample. Using smoothed and background-corrected data tends to obscure diffraction from very fine and poorly ordered CDDs.

2.3.2. *Preferred orientation*

Crystallographic orientation of particles can affect intensity as much as any other parameter, up to 100%. Particles having a perfect cleavage or acicular shape are most prone to preferred orientation. Finer particles are prone to orient because they generally are more equant. Mixing platy with equant particles reduces proneness to orient. For example, the use of an internal standard consisting of 20% or more equant particles can greatly decrease the tendency for platy crystallites like illite and kaolinite to orient.

2.3.3. *Sample homogeneity*

It may be hard to achieve when mixing is dry and a minor component is involved. Heterogeneity affects

sample transparency and counting statistics. Wet mixing improves homogeniety and lessens the generation of fine particles.

2.3.4. Average mass attenuation coefficient, $\bar{\mu}$

This factor applies to polycomponent powders. It refers to the average mass attenuation coefficient of a mixture [7], in accordance with the recommendation of the International Commission on Radiation Units [18]. The symbol $\bar{\mu}^*$ has been used for the mass absorption coefficient of a polycomponent sample [19]. Also used is the symbol $\mu_t = \Sigma \mu_i w_i$ where μ_t is total mass absorption coefficient of the powder, μ_i is the mass absorption coefficient for the pure element i, and w_i is the weight fraction of the element i [6]. As currently used, the symbol $\bar{\mu} = \bar{\mu}^* = \mu_t$. Quantification methods not using an internal standard require accurate determination of this mass absorption coefficient. As $\bar{\mu}$ decreases, sample transparency increases, allowing greater penetration of X-rays and increasing the proportion of non-surficial particles irradiated, which increase sample displacement errors.

2.3.5. Microabsorption

This factor comes into play when two or more substances having different mass absorption coefficients are mixed. It is higher when a component has a high absorption coefficient. This factor cannot be ignored when powders are coarse, but is negligible when powders are finer than 5 μm.

2.3.6. Size of sample surface exposed to X-rays

The surface exposed to X-rays is not the same for all diffractometers. Typical sample surface dimensions are 26×26 mm, with the outside dimensions of the sample holder being 30×30 mm. The size of the irradiated surface varies with divergence slit width and 2Θ (Fig. 2). For quantitative analysis, the largest surface that can intercept the beam should be used. If the width of the irradiated area becomes too large, flat specimen error might become significant.

2.3.7. Thickness of the powder

Thickness should be great enough to prevent the X-ray beam from passing through it. The thickness necessary to reduce the incident beam to 1/1000th of its initial intensity is:

$$e^{2\bar{\mu}t/\sin\Theta} = 1000$$

or

$$t = 3.45\sin\Theta/\bar{\mu},$$

where $\bar{\mu}$ is the average mass attenuation coefficient of the sample, and t is its thickness, in microns. Table 3 gives requisite powder thickness for various values of μ, 2Θ, and porosity. The weight of powder (mg)

Table 3
Examples of powder thickness (μm) required for attenuation of a cuK$_\alpha$ beam to 0.5, 0.01 and 0.001 times incident intensity as a function of 2Θ

Attenuation factor		0.5				0.01				0.001			
Porosity		solid	0.9	0.8	0.7	solid	0.9	0.8	0.7	solid	0.9	0.8	0.7
	4°	2.1	2.4	2.7	3.0	14.1	15.7	17.7	20.2	21.2	23.6	26.5	30.3
Gibbsite	20°	10.6	11.8	13.2	15.1	70.4	78.2	88.0	100.5	105.6	117.3	131.9	150.8
μ=56.8 cm^{-1}	40°	20.9	23.2	26.1	29.8	138.6	154.0	173.3	198.0	207.9	231.0	259.9	297.0
$\bar{\mu}$=24.2 cm^2 g^{-1}	80°	39.0	44.0	49.0	56.0	261.0	289.0	326.0	372.0	391.0	434.0	488.0	559.0
	4°	1.3	1.4	1.6	1.8	8.3	9.3	10.4	11.9	12.5	13.9	15.6	17.8
Quartz	20°	6.2	6.9	7.8	8.9	41.4	46.0	51.8	59.2	62.2	69.1	77.7	88.8
μ=96.5 cm^{-1}	40°	12.3	13.7	15.4	17.6	81.6	90.7	102.0	116.6	122.4	136.0	153.0	174.9
$\bar{\mu}$=36.4 cm^2 g^{-1}	80°	23.1	25.7	29.9	33.0	153.4	170.5	191.8	219.2	230.1	255.7	287.6	328.7
	4°	0.1	0.1	0.1	0.2	0.7	0.8	0.9	1.0	1.1	1.2	1.3	1.5
Hematite	20°	0.5	0.6	0.7	0.8	3.6	4.0	4.34	5.1	5.3	5.9	6.7	7.6
μ=1124.4 cm^{-1}	40°	1.1	1.2	1.3	1.5	7.0	7.8	8.8	10.0	10.5	11.7	13.1	15.0
$\bar{\mu}$=216.2 cm^2 g^{-1}	80°	2.0	2.2	2.5	2.8	13.2	14.6	16.5	18.8	19.7	21.9	24.7	28.2

needed for this thickness, for a given 2Θ, is the area of the sample surface (mm^2) × thickness (μm) × density of the powder × 10^{-3}. For example, 35 mg of quartz in a typical sample holder is enough to completely attenuate the beam at 25°2Θ.

2.3.8. Surface of the powder

The surface should be flat and smooth. Any flexure, roughness, or porosity contributes to transparency and sample displacement errors. For the (101) peak of quartz at 26.7°2Θ, μ=96.5, porosity 30%, for example, more than half the diffracted intensity is from the uppermost 9 μm thickness of powder, while a peak at 50°2Θ, with μ and porosity the same, gets half of its intensity from the uppermost 20 μm thickness.

2.3.9. Powder packing and transparency

The high porosity of most powders requires packing to reduce sample transparency, but excessive packing should be avoided. It might induce preferred particle orientation, a major source of error, and even change the inherent properties of some phases. Hardly any powder will have total voids less than 25% if gently packed or less than 15% if tightly packed. Loose powders may have 50% voids or more, depending upon the material. The recommended mounting method described below is a compromise between the advantages and disadvantages of packing.

2.3.10. Methods for making powder mounts

The smear mount, the cell mount, and the backpacked cell mount are perhaps the three most commonly used. The likelihood of preferred orientation of inequant particles is greatest in the smear mount and least in the backpacked cell. The best general purpose method for preparing a backpacked cell is described below in section 4.4.

2.3.11. Choice of internal standard

Five oxide powders have been prepared by the National Institute of Standards and Technology, Gaithersburg, Maryland, and made available for use as certified internal standards for quantitative powder XRD analysis. They are relatively inert, properly sized, and accompanied by data on lattice parameters, relative intensities, and particle size distribution. One of them is a suitable standard for the analysis of virtually any solid phase. Optimally, the chosen standard should have a strong diffraction peak near to but not interfering with that of the analyte, nor with that of any other powder component.

2.4. Parameter summary

The more important parameters in quantitative XRD analysis are (1) CDD size distribution, (2) counting statistics, (3) preferred orientation, (4) inherent properties of the analyte, (5) how the sample is prepared, (6) how the sample is mounted, and (7) how the raw data are reduced. Another 18 factors, more or less, can significantly affect accuracy. Several parameters are associative and interrelated. Counting statistics, for example, may be regarded as a net factor resulting from the interplay of a subset of other factors: generator power, scan rate, chopper increment, peak intensity, and background intensity. Likewise, preferred orientation involves another subset consisting of the inherent properties of the analyte and several factors relating to the method used to make and mount the powder. Inherent properties of the analyte involve still another subset: coherent domain size, absorption, structure factor, and multiplicity. In some combinations, the effects of individual factors are additive, in other cases countering. A factor in one group may change a factor in another. For example, CDD size can be changed by preparational factors like grinding and sizing. A comparison of the parameters listed in Table 1 with those explicitly considered in published quantitative measurements shows that one or more important factors have been neglected in otherwise very careful work.

The lack of scatter of points along a calibration curve is not always a good indication of analytical accuracy, because data smoothing, averaging, or other treatments can obscure raw data disparities which otherwise might indicate that a critical parameter had been neglected during intensity measurements.

Relatively easy checks can be made for the likelihood of significant error from major intensity-influencing factors. For counting statistical error, the total number of counts used to establish peak and background intensities can be examined. To check the possibility of error from preferred orientation, the

sample mount can be rotated and X-rayed again or remade and X-rayed. For possible error due to CDD size, a careful check can be made for line broadening, using the raw data file. A better check can be made by lattice imaging.

3. Brief review of quantitative methods

Since the 1920's, when practical application of X-rays to phase quantification began, several methods have been developed. They can be categorized in four groups, those using no standards, external standards, internal standards, or multiple additions of analyte. The basic equation expressing the relation between the quantity of a phase and its diffraction intensity, for all groups, is:

$$I_p = K_p w_p / \bar{\mu},$$

where I_p is diffraction intensity from component p, w_p is weight fraction of p, K_p is a constant which depends upon the inherent properties of p, the reflection being used, and the experimental arrangement, and $\bar{\mu}$ is the average mass attenuation coefficient of the powder [18,7]. The same equation has been presented in the form [19]:

$$I_p = K_p(w_p/\rho_p)/\Sigma w_p \mu_p$$

where ρ_p is the density of p and $\Sigma w_p \mu_p$ is the average attenuation coefficient. In the basic equation above, ρ_p is included in the constant K_p. For a mixture of substances p,q,r....in weight proportions of w_p, w_q, w_r...., the average attenuation coefficient can be written: $\bar{\mu} = w_p\mu_p + w_q\mu_q + ...$, summing over all components.

Matrix absorption effects are eliminated by the internal standard methods. A calibration curve is established by plotting $w_s(I_p/I_s)$ against w_p, where s refers to the internal standard. When the same proportion of internal standard is added to each sample:

$$I_p/I_s = Kw_p, \text{ and } wp = K'(I_p/I_s), \text{ where } K' = 1/K.$$

For the Reference Intensity Ratio (RIR) method [4,5]:

$$w_p = w_s(I_p/I_s)/(I_{s\,50/50}/I_{p\,50/50}),$$

or

$$w_p = C(I_p/I_s), \text{ where } C = w_s(I_{p\,50/50}/I_{s\,50/50}).$$

Good examples of quantitative analysis by XRD are: without an internal standard [6,8]; with an internal standard [8,4,5]; by known additions of analyte [9]. XRD has been used with polarization and electron microscopy [2,3], IR spectrometry, thermal analysis, and other methods, complimentarily, to accomplish higher reliability in quantitative analysis. A good general review of all XRD methods is in [7].

Though quantitative analysis without standards has been demonstrated [20,21], it is neither comparable to other methods in acccuracy nor general applicability. Mass absorption coefficient correction methods and internal standard methods appear to be equivalent in accuracy [8]. For general applicability and highest accuracy, however, they have to be buffered by information from other sources, as espoused by Bardossy and others [2,3], and as indicated by the parameters in sections B and C of Table 1. An accurate estimate of quartz below 0.1% by the method of known additions of analyte requires 2–6 hours [9]. For example, in the ADDENDUM, the RIR method [4] was used.

4. Sample preparation for powder XRD

4.1. Introductory comments

The importance of sample preparation has been recognized long time ago. A half century ago, microabsorption was described [22]. Forty years ago thermal shock was used to increase diffraction intensity. However, the effects of sample preparation have not been investigated in the same detail as X-ray generation, diffraction, and electronic measurement. A reason for this is that sophisticated equipment for comminution and size fractionation of materials and direct observation of submicroscopic CDDs has been slower to develop. Current quantification methods rely on particle size rather than CDD size as the gauge of fineness. Improvements in the ease and accuracy of CDD size measurement now enable consideration of all the factors in Table 1. Careful use of available comminution and sizing equipment

enable significant improvement in routine XRD quantification, even without the use of TEM.

4.2. Preliminary handling of solid or coarsely particulate samples.

If the sample as received is small, up to several pounds, and is sand or finer, a representative portion small enough for final grinding and/or mixing with an internal standard can be obtained by splitting with a Jones Splitter, Soiltest Sample Splitter model CL284, or a mix-and-quarter routine. If the sample is solid or coarsely particulate, it is comminuted, preferably by impact crushing, and then split. When very bulky material is to be analyzed, grab sampling or other means may be the initial step.

4.3. Obtaining optimal powder for XRD

In the ideal powder all particles are equant, unstrained, ≈5–0.2 microns in diameter, randomly oriented, and tightly packed.

Probable error of intensity measurement increases with the proportion of particles coarser than 5 microns, due to primary extinction and to the decreasing total number of particles in the mount. Because of the latter, different orientations are represented by fewer particles and intensity measurements are less reproducible. Particles with diameters <0.2 micron cause a systematic reduction in peak intensity. This trend continues as size decreases, down to about 0.005 micron (4–5 unit repeats), where peak intensity approaches zero.

While customary sizing of material is concerned with particle size, CDD size is the critical dimension for XRD work. Optimal particle sizing can be the first step. The next step is to find out whether or what proportion of the optimally sized particles consist of even finer CDDs. A particle size distribution is only a first approximation of CDD size distribution.

Figure 9 shows how a diffraction peak lowers and broadens with decreasing N. A peak can hardly be distinguished by X-rays when N is <5, especially when the compound/mineral is a small proportion of the sample. Generally, 0.1 micron CDDs give significant line broadening in the back reflection region and 0.2 micron CDDs do not. Diffractometers use the forward reflection region, so nearly all CDDs 0.2 micron and coarser do not show line broadening.

How the sample is ground to optimal powder depends upon attributes of its components. Examination with a binocular microscope generally can reveal whether a powder consists of one component or several, whether the components have physical differences that might affect their grindability, as hardness, cleavage, or shape, and roughly how particle size already varies. A powder that does or might contain more than one component should be totally reduced to the desired size, to avoid compositional fractionation. When the components differ considerably, grinding might have to be periodically interrupted to split off the finer fraction in order to minimize the generation of −0.2 micron particles. Finally, fine fractions have to be remixed to maintain the sample's representativeness.

Wet milling, as in a McCrone Micronizing Mill, is perhaps the best way to grind a powder or mix polyphase material [16]. Because the amount of energy required for comminution generally increases with decreasing size, coarser particles tend to grind preferentially. Milling can be stopped before a significant quantity of ultrafine debris has been produced. Wet milling not only produces fewer ultrafine particles but also minimizes lattice strain. Using a volatile liquid like alcohol or acetone rather than water in the mill accelerates grinding and mixing. A convenient procedure with a McCrone Micronizing Mill is to grind about 3 g of powder in 4 ml of ethanol for 7 min and wash the mill between grinds with 10 ml of ethanol, about 15 s of agitation, repeated twice.

The fractionation of micron-size and finer particles with existing equipment can be laborious. For sake of efficiency and cost, a compromise on accuracy sometimes is acceptable. With a Gilsonic Autosiever a powder can be conveniently split at 10 microns. By interrupting the wet micronizing grind, as necessary, to split off the <10 micron fraction, a powder can be produced with an upper size limit that is acceptable and a minimal proportion of particles finer than 0.2 micron. A final measurement by Stokes Law settling can show whether there are particles finer than 0.2 micron. All instruments now sold for measuring the size distribution of submicron particles are subject to increasing error as size decreases. For

more reliable measurement, prepare a mount of unflocced particles and measure size directly with SEM.

For homogeneous mixing of standards or of analyte with an internal standard, wet mix in a micronizing mill. Underlying the practical procedures above, is the assumption that particle size distribution is the same as CDD size. Sofar, as this assumption is unjustified, the procedure has to be modified if accurate XRD quantification is to be achieved.

To check on whether preferred orientation exists, accumulate 100 000 counts at the top of a strong peak, preferably at a 2Θ low enough for most of the sample to be irradiated, then remeasure after sample rotation. If the stage cannot rotate, remove the sample, rotate 90°, and replace it before remeasuring. A change in peak intensity of more than 10% after rotation suggests too much preferred orientation or unacceptabe sample heterogeneity.

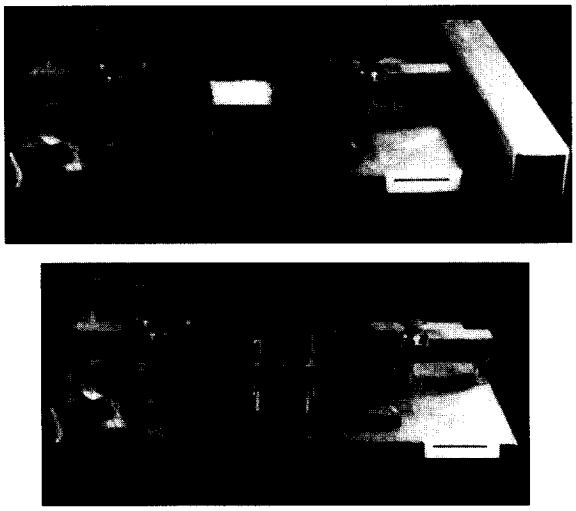

Fig. 10. Paraphernalia for making a backpacked powder mount. The black line at the right is 2.54 cm long.

4.4. Mounting the powder for XRD

Sprinkling fine powder onto a flat surface is much less apt to orient particles than shearing or surface packing. Sprinkling and backpacking, combined, may eliminate preferred orientation if the powder components lack a perfect cleavage and are even moderately inequant, particularly if the mass absorption coefficient is moderate or low, when fewer irradiated particles will be surficial.

To use the recommended mounting procedure, sprinkle the sample into a machined square metal holder clamped to a flat glass surface (Fig. 10), enough powder to completely attenuate the direct beam (Table 3). For better sprinkling, place a clean 60 mesh screen over the sample holder, dump the powder onto the screen and tap it so that the powder falls through. Then gently insert the vertical square metal die into the sample holder; lower gently to lightly pack the powder. Remove the die and fill the holder with cellulose. Place the glass plate with the filled holder onto the stage of a press, position the metal die atop the cellulose and apply a pressure of 200–300 psi. After 10 s, release the pressure, lift the die vertically from the mount, and unclamp the mount from the glass surface, taking care to avoid any lateral movement that might orient surface particles. This produces a mounted powder with reduced porosity, an even flat surface, and generally little preferred orientation.

5. X-ray data collection and interpretation

Expedient sample processing – grinding to <200 mesh (75 microns) with little regard for CDD size or counting statistics, collecting XRD data by rapid scans, routine smoothing of raw data, and use of default choices for background subtraction and intensity measurement – might be acceptable for indiscriminant qualitative analysis, but not for quantitative work, particularly not when the concentration of analyte is low. For best accuracy, consider all 33 parameters in Table 1, along with any information needed from other sources to evaluate CDD size distribution and mounting of the powder.

6. Addendum: Routine quantification of quartz by powder XRD

6.1. Selection of standards

The following reference materials were used to prepare standards:

(a) α-quartz, from Jim Hubbard, Materials Analytical Services, Atlanta; same as beach sand from Standard Sand and Silica, Davenport, Fla.
(b) Silica glass made by General Electric in early 1960s for use as a refractory.
(c) α-Al_2O_3 from National Institute of Standards and Technology.

α-Al_2O_3 was chosen as a standard because one of its strong lines, (012) at 25.54°2Θ, is close to the strongest line of quartz, (101) at 26.66°2Θ. Silica glass was chosen as filler for the standards because it simulates the background commonly found in fly ash and other common industrial materials. One standard was prepared with a 0.5/0.5 weight fraction for α-Al_2O_3/quartz. In the other standards, the weight fraction of α-Al_2O_3 was 0.1.

6.2. Consideration of intensity-affecting parameters

All parameters in Table 1 were considered, consistent with accurate intensity measurement of the (012) α-Al_2O_3 and (101) quartz lines. The analyte being well ordered quartz, structure factor, multiplicity, long-range and short-range order could be disregarded. The absorption factor, μ, could be neglected because of diffractometer geometry. Primary and secondary extinction and microabsorption were neglected because powder particles <10 mi- 10 microns in diameter were used. Preferred orientation was neglected because quartz fractures conchoidally and fine particles tend toward equant shape; likewise, α-Al_2O_3 fractures conchoidally to unevenly and tends toward equant shape. Mass attenuation coefficient, $\bar{\mu}$, could be neglected because an internal standard was used. Minimization of errors from other parameters was achieved by using the best procedures described above for preparing and mounting powders, except to demonstrate error from these sources.

6.3. Powder preparation and mounting

Three sets of samples were prepared from the same reference materials. One set was dry ground and mixed by hand with a mortar and pestle. The second set was dry ground and mixed in a SPEX grinder-mixer mill #8000. Both sets of powders were ground to pass 200 mesh. The third set was prepared by wet milling in a McCrone Micronizing Mill, as detailed above. For this set, the upper size limit was checked with a Gilsonic Autosiever which can reliably split at 10 microns, as verified with SEM. More tedious measurement of size distribution below 0.2 micron was not undertaken because the crystalline components of these mixes respond to comminution similarly and the selected grinding procedure minimizes production of <0.2 micron particles.

The backpacked mounting procedure recommended above was used for all three sets of samples, to assure a flat, even surface and reduced sample porosity. Three XRD mounts were prepared of each sample in each set.

6.4. Selection of systematic parameters and data collection

A SCINTAG XDS-2000 diffractometer with Θ-Θ configuration, solid state detector, and copper tube was used. Fixed slits: divergence 1° and 2°, receiving 0.5° and 0.3°. Generator power: 45 kV, 40 mA. Continuous scan, $K_{\alpha 2}$ stripping, no Lorentz-Polarization correction, and no background correction, followed by determination of peak height and background from the *.RD file. A quick and relatively accurate procedure is to scan the 24–28°2Θ range at 0.2°2Θ min^{-1} with 0.01° chopper increment and then determine peak height and background from the *.RD file. If background cannot be approximated by a straight line over the entire 24–28°2Θ range, a scan can be made over a wider range to identify the interference and overcome it.

Better quantification of the mixes described above is obtained by scanning the 24.6–27.6°2Θ range at 0.2°2Θ min^{-1} with 0.05° chopper increment and using the *.RD file and deconvolution software provided with the system, with background averaged over the background trace, to determine net intensity. This parameter selection is a compromise between time required for the analysis and precision. Precision can be improved by a slower scan and/or a smaller chopper increment.

6.5. Treatment of XRD data

A 15 min run as specified above yields a *.RD file from which peak intensities based on height or area

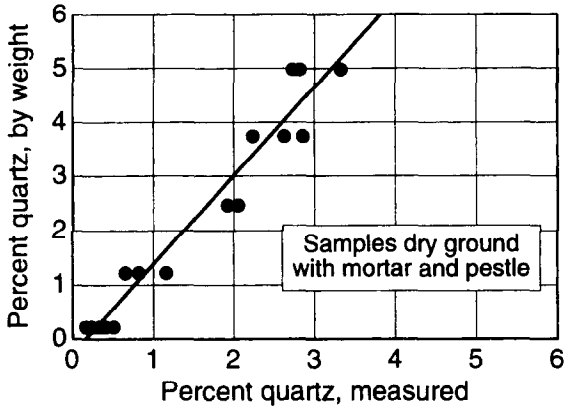

Fig. 11. Data from first set of samples (dry ground with mortar and pestle). Percent quartz by weight versus percent calculated by the RIR method, using net intensities after automatic background correction. Net intensities from the PFLIST program.

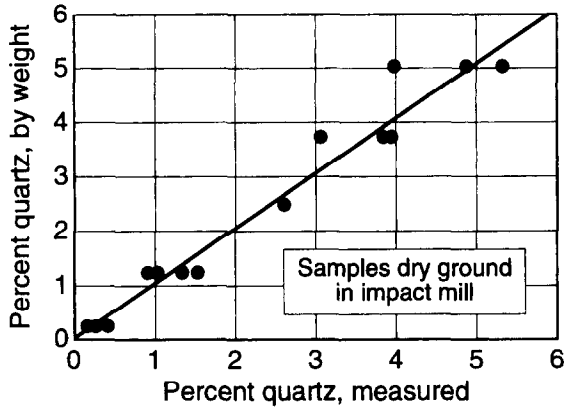

Fig. 12. Data from second set of samples (dry ground and mixed in a SPEX impact mill). Percent quartz by weight versus percent calculated by the RIR method, using intensities obtained by manual measurement of peak height and background on color charts of the raw data files.

of the peak, with or without background correction, can be obtained.

For the first set of samples, net peak intensities were calculated by the PFLIST program after automatic background correction and percent of quartz was calculated by the RIF method. Fig. 11 is a plot of actual versus measured percent quartz.

For the second set of samples, peak intensities and background were measured manually on raw data prints; average background was subtracted from each peak to obtain net intensity which then was used to calculate percent of quartz. Fig. 12 shows the results. Figs. 11 and 12 demonstrate the difficulty in achieving sample homogeneity by dry mixing-grinding.

For the third set of samples, net intensities were obtained from the raw data files in three ways: by using the SCINTAG deconvolution program, a non-linear least-squares peak-fitting routine and Gaussian profiles, with background set at zero (Fig. 13), by using the same deconvolution program with background set at the average of the background trace (Fig. 15), and by manual measurement of peak height and background on raw data prints (Fig. 14).

Only Figs. 12 and 15 show the most direct relationship measured and actual percent of quartz. The scatter of points in Fig. 12 is attributable to insufficient grinding (some quartz particles were too coarse) and poor (dry) mixing of components. The small scatter of points in Fig. 15 at low concentra-

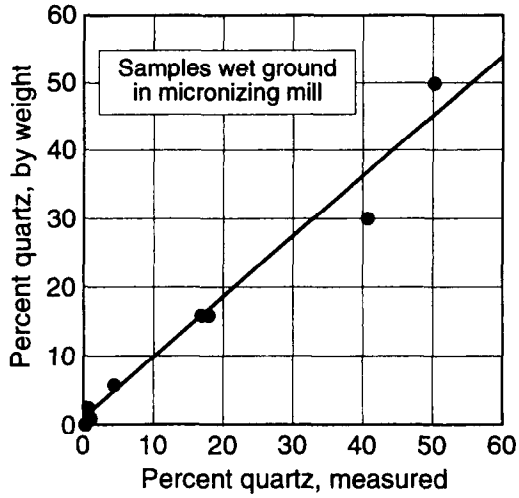

Fig. 13. Data from the third set of samples (wet milled and mixed in a McCrone Micronizing mill). Net intensities obtained by deconvoluting the raw data with background set at zero.

tions of quartz can be decreased by more careful sizing of powder particles and by increasing the time of wet mixing. Measurement error when quartz concentration is below 5% can be significantly decreased by longer counts, commensurate with desired precision (see Fig. 4).

If there is a 1:1 relationship between measured diffraction intensity and the proportion of quartz in the sample, the diagonal line in Fig. 15 should pass

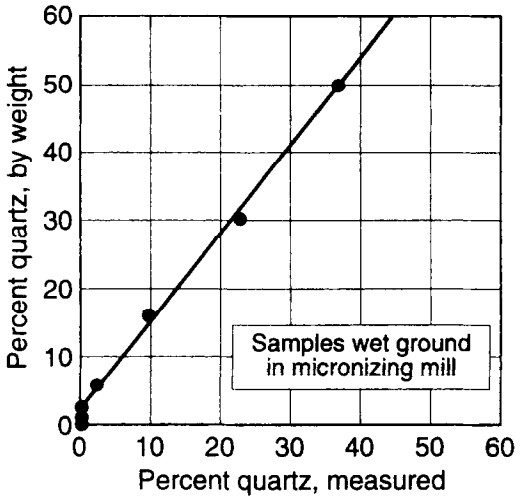

Fig. 14. Data from the third set of samples. Net intensities obtained by manual measurement of peak height and background on color charts from raw data files.

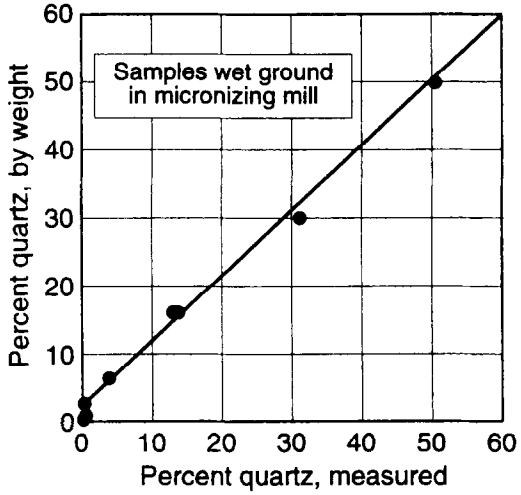

Fig. 15. Data from third set of samples. Net intensities obtained by deconvoluting the raw data files, with background set at the average of the background trace.

through coordinates 0,0 and 60,60, as it does in Fig. 15. Actual and measured values agree closely with such a line when quartz is >30% of the sample, but depart from the line more and more as quartz content decreases. Measurement uncertainty during routine work increases rapidly as quartz content drops below a few percent.

7. Conclusions

The shortest, accurate way to quantify quartz by the procedure adopted here is to make a single scan of the 24.6–27.6°2Θ range, using the specified parameters, and then use the deconvolution program, with background set on the average of the background trace, to measure peak intensities.

Other procedures as adopted by [8,9] yield the same order of precision when applied to well ordered quartz with optimal CDD size in a standard matrix, when other intensity-affecting parameters are about the same. Particularly important are (1) total counts accumulated at each point on the curve used to establish peak height or area, (2) assurance that all CDDs of the analyte are within the size range of 5–0.2 microns, (3) accounting for background, and (4) homogenization of the X-rayed samples. For the method of known additions, adequate sample homogenization must be not only assured at the start but also maintained during the mixing of each addition of analyte.

Similar analytical precision cannot be expected when different materials are analyzed by the same procedures unless differences in the matrix of the analyte are taken into account, CDD size and size distribution of the analyte are adequately evaluated, and other parameters affecting intensity measurement are optimized.

With the parameter optimizations chosen in this example, which involves a common matrix and a single analyte easily prepared for optimal CDD size and minimal preferred orientation, the analyte can be reliably measured at a concentration of 0.1%.

Other polymorphs of crystalline silica may be analyzed with similar precision if none of their CDDs are finer than 0.2 micron (generally not the case), if matrix effects are taken into account, and all other intensity-affecting parameters are optimized.

To the 14 forms of crystalline silica generally listed [24] the mineral moganite should be added [15].

Familiarity with all phases in a sample to be measured can minimize errors from peak interferences and fine CDDs. Unless the mineralogy of the matrix is known, precise calibration does not assure accurate determination of the analyte.

Crystalline silica polymorphs consisting of CDDs finer than 0.1 micron should not be regarded as

reliably quantifiable by published procedures at concentrations several times greater than 0.1% or even when concentration exceeds several percent, unless a supplemental method, as high resolution TEM, is utilized.

References

[1] W.J. Miles, Crystalline Silica Panel Workshop, Intertech International Conf. Washington, DC, 1992.
[2] G. Bardossy, L. Proc. 2nd Conf. VAMI and FKI experts, 1972, 27-42.
[3] G. Bardossy, L. Bottyan, P. Gado, A. Griger and S. Sasvari, Min. Soc. Amer., 65 (1980) 135–141.
[4] F.H. Chung, J. Appl. Cryst., 7 (1974) 519–525.
[5] F.H. Chung, J. Appl. Cryst., 8 (1975) 17–17.
[6] R.J. Parker, Min. Mag., 42 (1978) 103–106.
[7] G.W. Brindley, Min. Soc. Monogr. No. 5, London, 1980, p. 495.
[8] J.R. Carter, M.T. Hatcher and L. DiCarlo, Anal. Chem., 59 (1987) 513–519.
[9] T.L. Salter and W.E. Riley, Anal. Chim. Acta, 289 (1994) 49–55.
[10] W.J. Miles, Anal. Chim. Acta, 286 (1994) 97–105.
[11] D.L. Bish and J.E. Post, Min. Soc. Amer., Reviews in Mineralogy, Vol. 20, 1989.
[12] B.D. Culity, Elements of X-ray diffraction, Addison-Wesley, Reading, MA, 1978.
[13] R.C. Reynolds, Amer. Mineralogist, 50 (1965) 990–1001.
[14] International Tables for X-ray Crystallography, Vol. 11, 1972, 241–264.
[15] P.J. Heaney and J.E. Post, Science, 255 (1992) 41–43.
[16] B.H. O'Connor and W.J. Chang, X-ray Spectrometry, 15 (1986) 267–270.
[17] P.J. Heaney, D.R. Veblin and J.E. Post, Amer. Mineralogist, 79 (1994) 452–460.
[18] J.H. Hubbell, W.H. McMaster , N.K. Del Grande and J.H. Mallett, International Tables for Crystallography, The Kynoch Press, Birmingham, England, 1974, Vol. 5, pp. 47–70.
[19] H.P. Klug and L.E. Alexander, X-ray diffraction procedures, Wiley, New York, 1974.
[20] A.L. Salyn and V.A. Drits, Proc. Int. Clay Conf., Madrid, 1972, 797–806.
[21] L.S. Zevin, J. Applied Crystallogr., 10 (1977) 147–150.
[22] G.W. Brindley, Phil. Mag., 36 (1945) 342–369.
[23] V. Trunz, Clays and Clay Minerals, 1976, pp. 84–87.
[24] J.M. Elzea, I.E. Odem and W.J. Miles, Anal Chim. Acta, 286 (1994) 37–47.
[25] G.P. Tomaino, Anal. Chim. Acta, 286 (1994) 75–80.
[26] Special issue of papers presented International Symposium on issues and controversy: The measurement of crystalline silica. H.L. Pardue (Ed.), Anal Chim. Acta, Vol. 286, 1994.